



Universiteit  
Leiden  
The Netherlands

## **In vitro and in vivo delivery of functionalized nanoparticles via coiled-coil interactions**

Yang, J.

### **Citation**

Yang, J. (2016, December 1). *In vitro and in vivo delivery of functionalized nanoparticles via coiled-coil interactions*. Retrieved from <https://hdl.handle.net/1887/44712>

Version: Not Applicable (or Unknown)

License: [Licence agreement concerning inclusion of doctoral thesis in the Institutional Repository of the University of Leiden](#)

Downloaded from: <https://hdl.handle.net/1887/44712>

**Note:** To cite this publication please use the final published version (if applicable).

Cover Page



Universiteit Leiden



The handle <http://hdl.handle.net/1887/44712> holds various files of this Leiden University dissertation

**Author:** Jian Yang

**Title:** In vitro and in vivo delivery of functionalized nanoparticles via coiled-coil interactions

**Issue Date:** 2016-12-01

# Chapter 3

## Application of Coiled-Coil Peptides in Liposomal Anticancer Drug Delivery Using a Zebrafish Xenograft Model

Jian Yang, Yasuhito Shimada, René C. L. Olsthoorn, B. Ewa Snaar-Jagalska,

Herman P. Spaink, and Alexander Kros

*Chapter 3 has been published in ACS Nano*

ACS Nano **2016**, 10, 7428–7435; DOI: 10.1021/acsnano.6b01410.  
Supplementary Tables are available online.

### ABSTRACT

The complementary coiled-coil forming peptides  $E_4$  [(EIAALEK)<sub>4</sub>] and  $K_4$  [(KIAALKE)<sub>4</sub>] are known to trigger liposomal membrane fusion when tethered to lipid vesicles in the form of lipopeptides. In this study, we examined whether these coiled-coil forming peptides can be used for drug delivery applications. First, we prepared  $E_4$  peptide modified liposomes containing the far-red fluorescent dye TO-PRO-3 iodide ( $E_4$ -Lipo-TP3), and confirmed that  $E_4$ -liposomes could deliver TP3 into HeLa cells expressing  $K_4$  peptide on the membrane (HeLa-K) under cell culture conditions in a selective manner. Next, we prepared doxorubicin-containing  $E_4$ -liposomes ( $E_4$ -Lipo-DOX), and confirmed that  $E_4$ -liposomes could also deliver DOX into HeLa-K cells. Moreover,  $E_4$ -Lipo-DOX showed enhanced cytotoxicity towards HeLa-K cells compared to free doxorubicin. To prove the suitability of  $E_4/K_4$  coiled coil formation for *in vivo* drug delivery, we injected  $E_4$ -Lipo-TP3 or  $E_4$ -Lipo-DOX to zebrafish xenografts of HeLa-K. As a result,  $E_4$ -Liposomes delivered TP3 to the implanted HeLa-K cells, and  $E_4$ -Lipo-DOX could suppress cancer proliferation in the xenograft when compared to non-targeted conditions (*i.e.* zebrafish xenograft with free DOX injection). These data demonstrate that coiled-coil formation enables drug selectivity and efficacy *in vivo*. It is envisaged that these findings are a step forward towards biorthogonal targeting systems as a tool for clinical drug delivery.

## INTRODUCTION

The design of anticancer drug delivery systems is of great interest, as many of the drugs in the clinic cause serious toxic side effects due to non-specific cytotoxicity outweighing the therapeutic effect. Therefore targeted drug delivery systems are being developed, for example micellar, liposomal and nanoparticle based drug formulations combined with peptide or surface-antibody targeting, photochemical internalization and ultrasound stimulation.<sup>1</sup> Of these, liposomes are the most clinically established nano-systems for drug delivery, e.g. doxorubicin (DOX)-containing liposomes.<sup>2, 3</sup> However these clinically approved drugs are non-targeted and rely on the enhanced permeability and retention effect, resulting in cardiotoxicity limiting their cumulative dose in cancer patients. To overcome this problem, liposomes have been conjugated with active targeting ligands, such as antibodies and cell penetrating peptides for target-specific drug delivery.<sup>4-6</sup> However, as these targeted ligands frequently interact with natural membrane receptors, liposome internalization occurs *via* endocytosis. As a result drug accumulation in early endosomes induces lysosomal activation, leading to rapid degradation of these drugs inside cells.<sup>7</sup> Furthermore, the number of these “cell-specific” receptors is limited, thereby putting restrictions on this type of drug delivery systems.

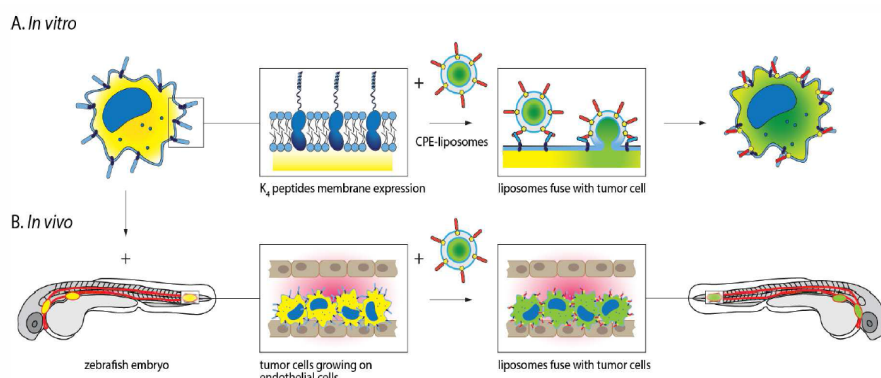
Therefore, it is important for the development of new drug delivery systems to avoid lysosomal degradation in order to enhance the delivery efficiency. We decided to design an artificial biorthogonal targeting system that might be able to target liposomes and other nanoparticles, more efficiently to the tissue of interest. In addition, this target system should also be able to enhance cellular uptake, preferentially in a nonendocytic manner. For this, synthetic coiled-coils are attractive candidates as a new targeting motif.<sup>8, 9</sup> Coiled-coil motifs are found in approximately 10% of all protein sequences in nature,<sup>10</sup> and many of these noncovalent peptide motifs play a vital role in the efficient transport of molecules across membranes. For example, in the process of HIV infection, viral entry into CD4-positive cells is accomplished by intramolecular coiled coil formation between helices of viral glycoprotein gp41.<sup>11</sup> In neuronal exocytosis, docking of transport vesicles to the target plasma membrane is mediated by the coiled coil formation of complementary SNARE protein subunits on the opposing membranes.<sup>12</sup> This forces the opposing membranes into close proximity, resulting ultimately in lipid mixing followed by pore formation and concomitant content transfer. These natural systems have inspired researchers to design drug delivery systems based on non-covalent binding of two macromolecules. To introduce bioactive compounds into the cytosol of the target cells, various non-natural coiled coils have been used to decorate nanoparticles,<sup>13, 14</sup> which in turn are complexed to DNA antisense oligonucleotides,<sup>15</sup> short interfering RNAs,<sup>16</sup> proteins,<sup>17</sup> drugs<sup>18, 19</sup> or vaccines.<sup>20</sup> Recently coiled-coil motifs have also been used in drug-free therapeutic systems.<sup>21, 22</sup>

In our previous study, we developed a fully synthetic membrane fusion system composed of a complementary pair<sup>23</sup> of lipidated coiled coil peptides, denoted K and E,<sup>18</sup> which are covalently linked to cholesterol anchors *via* a poly(ethylene glycol) linker, yielding lipopeptides CPK and CPE.<sup>24</sup> We demonstrated that this complementary lipopeptide pair was able to induce efficient fusion between liposomes.<sup>25</sup> <sup>26</sup> The E/K coiled coil formation is thought to be responsible for specific molecular recognition,<sup>27</sup> and recently membrane fusion between liposomes and cells without triggering endocytosis was achieved.<sup>28</sup> This system seems suitable for drug delivery, as the drug inside these liposomes avoid lysosomal degradation. While coiled coil formation induced membrane fusion has shown to be successful to deliver drugs *in vitro*, it has to be confirmed whether these synthetic peptide pairs are also functional in an *in-vivo* environment. In this study we therefore used a human cancer cell xenograft in a zebrafish embryo to investigate whether coiled coil formation can be used to specifically deliver drugs to tumor cells *in vivo*.

## RESULTS AND DISCUSSION

### E<sub>4</sub>-Liposomes Deliver TP3 to HeLa Cells That Genetically Express K<sub>4</sub> Peptide *in Vitro*

Our objective is to use a pair of complementary coiled coil forming peptides, E and K,<sup>28</sup> of which one is conjugated to a liposome to introduce chemicals into peptide-conjugated cancer cells in zebrafish (**Scheme 1**). The coiled-coil peptide E (EIAALEK)<sub>4</sub> was conjugated to a PEG<sub>4</sub> spacer (PEG = polyethylene glycol) and cholesterol linker, yielding lipopeptide CPE<sub>4</sub>, then inserted into the bilayer of liposome containing the fluorescent dye TO-PRO-3 iodide (TP3) (denoted E<sub>4</sub>-Lipo-TP3; **Scheme 1A**). TP3 is a DNA intercalating fluorescent dye and cell membrane-impermeant, and stains only DNA when it is actively taken up by live cells.<sup>29</sup> We previously confirmed that E<sub>4</sub>-Lipo-TP3 could deliver TP3 into the cytosol of HeLa cells that were pretreated with cholesterol-PEG<sub>4</sub>-K<sub>4</sub> (CPK<sub>4</sub>).<sup>28</sup> While targeted drug delivery under *in vitro* conditions was thus successfully achieved, demonstrating the *in vivo* functionality of these synthetic peptides would be a significant step forward. Due to the short turnover of membrane components in dividing cells, CPK<sub>4</sub> inserted in a cell membrane is not expected to remain throughout the zebrafish xenotransplantation setup and experiments.



**Scheme 1. Drug delivery by E4/K4 coiled-coil formation in cells (A) and zebrafish (B).**

For this reason, we created HeLa cells constitutively expressing a genetically encoded K<sub>4</sub> peptide on their cell membrane (denoted HeLa-K), by fusing it to the transmembrane domain of the human platelet-derived growth factor receptor (PDGFR-TMD).<sup>30</sup> The fusion protein is preceded by a mouse IgK-leader sequence for efficient secretion and localization on the cell membrane of the K<sub>4</sub>-fusion protein. Functional display of the K<sub>4</sub>-peptide on the outside of the cell membrane was verified in a binding experiment using a carboxyfluorescein-labeled E<sub>4</sub> peptide (Fluorescent E<sub>4</sub>; **Figure S1A**). Analogously to HeLa-K cells, we also created HeLa-E cells that potentially expressed E<sub>4</sub> peptide on their cell membrane and HeLa-ctrl cells, that only expressed the transmembrane domain of PDGFR. Fluorescently labeled CPK<sub>4</sub>-Liposomes (K<sub>4</sub>-Lipo-NBD) were bound to the cell membrane of HeLa-E cell (**Figure S2**), however fluorescent E<sub>4</sub> peptide was taken up by the cells (**Figure S1C**). Ono *et al.* already demonstrated that the positive charge of the K<sub>4</sub> peptide allowed nonspecific binding to negatively charged cell membranes.<sup>31</sup> Thus, we decided to continue with HeLa-K cells and E<sub>4</sub> peptide in the following study.

To investigate whether E<sub>4</sub>-liposomes could deliver TP3 to HeLa-K cells, HeLa-K cells were exposed to E<sub>4</sub>-Lipo-TP3 for 15 min. This resulted in the appearance of a bright TP3 signal in the cells (**Figure 1A**). Control experiments in which non-modified TP3-liposomes (Lipo-TP3; **Figure 1C**) or free TP3 (**Figure 1D**) were added to the HeLa-K cells showed less fluorescent signal in the cells. In addition, when E<sub>4</sub>-Lipo-TP3 was added to control HeLa cells (HeLa-ctrl), which express only PDGFR-TMD, also no TP3 signal was observed (**Figure 1B**). These results indicates that the coiled-coil formation between E<sub>4</sub> on the liposome and K<sub>4</sub> on the cell membrane lead to delivery of liposome contents into the cells in a selective manner.

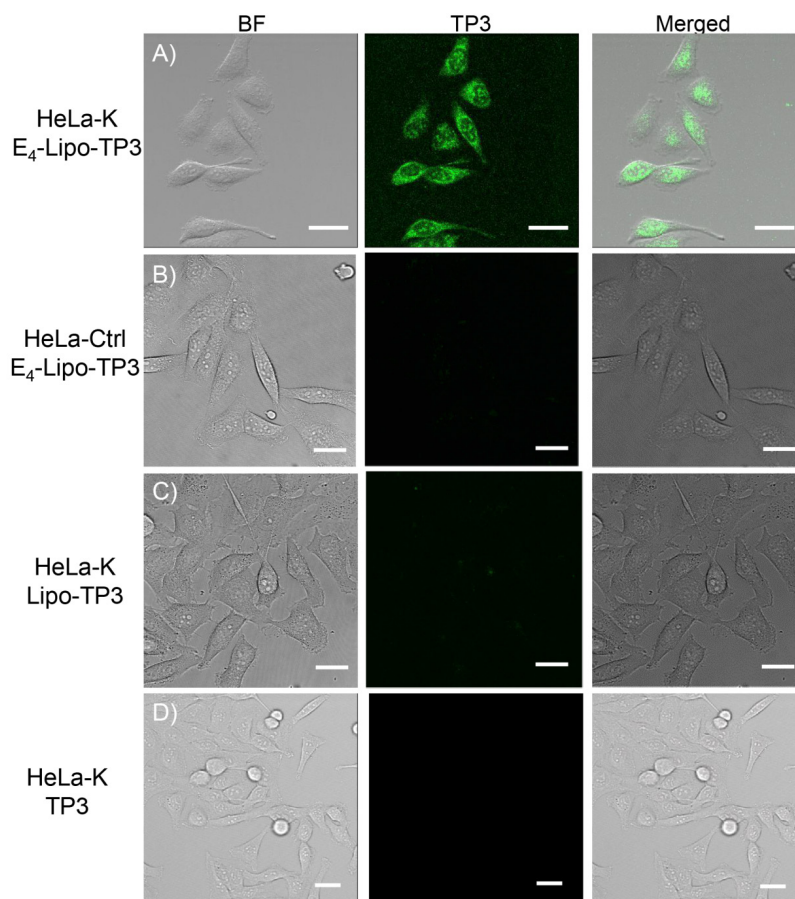


**Figure 1.  $E_4/K_4$  coiled-coil formation mediated TP3 delivery into the cytosol.** HeLa-K or control HeLa (HeLa-ctrl) cells were treated with 0.25 mM  $E_4$ -Lipo-TP3, Lipo-TP3 (without  $E_4$  peptide) or 2.5  $\mu$ M free TP3 for 15 min. After 3-time wash with culture medium, the cells were imaged.  $E_4$ -Lipo-TP3 can deliver the TP3 into HeLa-K cells (A), not into HeLa-ctrl cell (B). (C) Without  $E_4$  peptide, liposome could not deliver the TP3 into HeLa-K cells. (D) TP3 without liposome also could not deliver TP3. Green: TP3. The scale bar represents 25  $\mu$ m.

## $E_4$ -Liposomes Can Deliver TP3 in the Zebrafish Xenograft of HeLa-K Cells

Zebrafish is becoming a suitable model for characterization of nanoparticles against cancer, because of phenotypic and molecular conservation of cancer responses in zebrafish and human.<sup>32</sup> In addition, the transparency of zebrafish embryos enables to visualize fluorescently-labeled cancer cells and nanoparticles through their body



wall. To monitor the fate of the implanted cells in zebrafish, HeLa-K and HeLa-ctrl cells were labeled with a red fluorescent protein that was expressed from a transfected retroviral vector expressing tdTomato (tdTom). We injected the resulting HeLa-K-tdTom or HeLa-ctrl-tdTom cells into the blood circulation of zebrafish larvae at 48 hours post fertilization (hpf), according to the previous study.<sup>33</sup> We used transgenic zebrafish that express vascular-specific EGFP to visualize their vasculatures. Five hours post cell injection (hpi), we confirmed that the injected-cells accumulated in the caudal hematopoietic (CHT) region. Then,  $E_4$ -Lipo-TP3 or Lipo-TP3 was injected into the circulation from the posterior cardinal vein (CV). Immediately after  $E_4$ -Lipo-TP3 injection, no TP3 signal could be detected in the xenografts.

However, at 24 hpi, TP3 accumulation was observed in HeLa-K-tdTom cells in the CHT region (**Figure 2A**). Control experiments in which one of the two peptides was omitted (HeLa-K with Lipo-TP3 (**Figure 2B**) and free TP3 (**Figure S2A**), and HeLa-ctrl with  $E_4$ -Lipo-TP3 (**Figure S2B**) showed no TP3 uptake inside the cells. These results demonstrated that  $E_4/K_4$  coiled coil formation regulates delivery of liposomal cargo to the targeted cells in an *in vivo* setting.

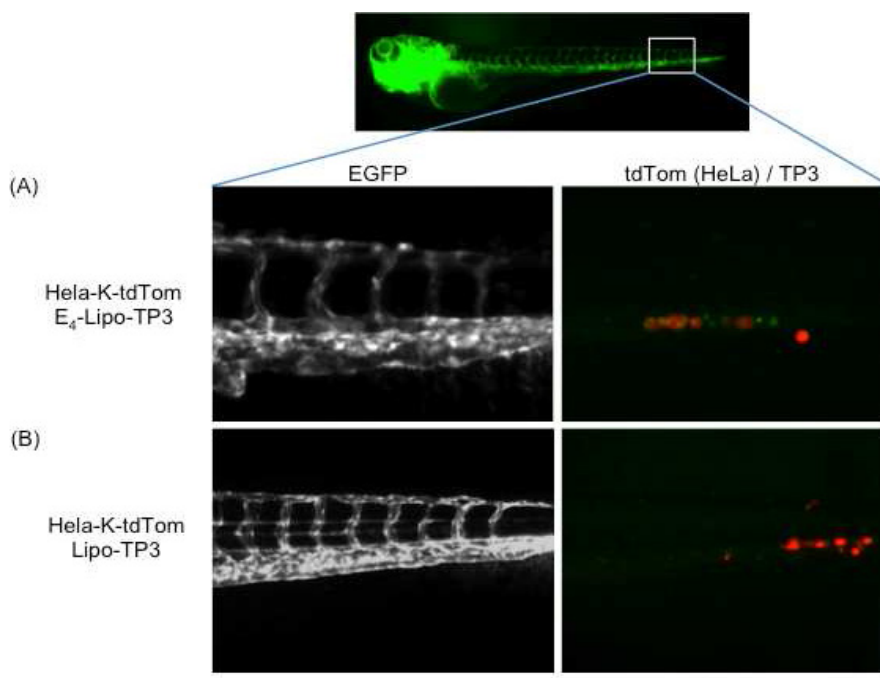


**Figure 2.**  $E_4/K_4$  coiled-coil formation delivers the content in the liposome to cancer cells in the xenograft zebrafish. HeLa-K cells (50-100 cells) were injected into the duct of Cuvier of 48 hpf zebrafish. Five hours after implantation (hpi), 1 nL of 1 mM  $E_4$ -Lipo-TP3 or Lipo-TP3 was injected from CV and imaged at 72 hpf. (A)  $E_4$ -Lipo-TP3 can deliver the TP3 to HeLa-K in the xenograft zebrafish, while (B) Lipo-TP3 could not. White, red and green indicates vasculatures, cancer cells and TP3, respectively. The scale bar represents 200  $\mu$ m.

### $E_4/K_4$ Coiled-Coil Formation Enhances DOX Cytotoxicity

Having demonstrated the feasibility of  $E_4/K_4$  system to target xenografted cancer cells in zebrafish, we next investigated whether our  $E_4$ -liposomes could also deliver an anticancer drug such as doxorubicin ( $E_4$ -Lipo-DOX). DOX has been commonly used as a routine anti-cancer drug in combined chemotherapy against a variety of tumors.<sup>34</sup> DOX interacts with DNA by intercalation and disruption of topoisomerase-II-mediated DNA repair, ultimately leading to cell death.<sup>35</sup> Noteworthy, DOX is a popular research tool due to its inherent fluorescence associated with the central anthracycline chromophore group. This allows visualization of DOX distribution in various tissues or cells *via* fluorescence imaging.<sup>36</sup> Indeed, we were able to visualize DOX-intake into HeLa-K cells. After 15 min incubation with 0.25 mM  $E_4$ -Lipo-DOX (1 mM DOX-containing  $E_4$ -liposome, equal to 0.25 mM free-DOX concentration), DOX fluorescent signal was already observed in the cytosol (**Figure 3A**). Five hours after washout of  $E_4$ -Lipo-DOX from the culture medium, DOX signal was increased (**Figure 3B**). Mohan *et al.* reported that the DOX fluorescence inside cells increases in a time-dependent manner because of the alternation of DOX's binding partners; DNA, histones and phospholipids.<sup>36</sup> Thus, we assumed that DOX-phospholipid and DOX-DNA-histone complexes would be detected after 15 mins incubation. In contrast, control experiments in which  $E_4$  peptide were omitted from the liposomes (HeLa-K with Lipo-DOX (**Figure S3A**) or using free DOX (**Figure S3B**) showed very low cellular uptake of DOX. As expected, free DOX was not taken up by HeLa-ctrl (**Figure S3C**) and HeLa-E cells (**Figure S3D**), similar to HeLa-K. We repeated the experiment in the presence of several well-known endocytosis inhibitors in order to study the pathway of cellular uptake (**Figure S6**). It was shown that uptake *via* endocytosis was the minor pathway, suggesting that fusion might be the major pathway. However additional studies are required to confirm this finding.

To investigate whether coiled-coil mediated delivery enhances the cytotoxicity of DOX, we treated HeLa-K cells with  $E_4$ -Lipo-DOX, Lipo-DOX or free DOX for 12 h. As a result, 1  $\mu$ M  $E_4$ -Lipo-DOX exhibited around 80% reduction in the number of HeLa-K cells, while free DOX had no measurable effect at the same concentration (**Figure 3C**). In addition, Lipo-DOX showed the same toxicity to that of free DOX to HeLa-K cells. This result indicates that  $E_4/K_4$  coiled-coil formation increases the cytotoxicity of DOX and reduces the dose required for the induction of cancer cell death. Interestingly, under non-targeting conditions with free DOX, HeLa-ctrl cells (**Figure S4**, open circle) seems more sensitive than HeLa-K cells (**Figure 3C**, open line). Membrane expression of  $K_4$  peptide might have some protective effects to the cells, however the  $IC_{50}$  of DOX against HeLa-ctrl and HeLa-K cells are similar, 4.0  $\mu$ M and 5.3  $\mu$ M, respectively.

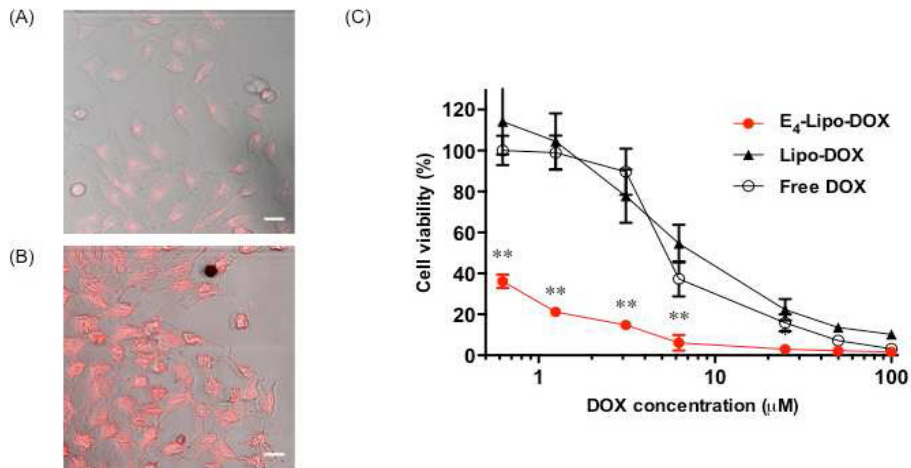


**Figure 3.  $E_4/K_4$  coiled coil formation promotes doxorubicin intake and cytotoxicity.** HeLa-K cells were incubated with 1 mM of  $E_4$ -Lipo-DOX (equal to 0.25 mM DOX) for 15 min, after 3-time wash with culture medium, the cells were imaged (A). After 5h, the cells were imaged again (B). Red indicates DOX. The scale bar represents 25  $\mu$ m. For images of negative controls, see supplementary Figure S3. (C) Cell viability after DOX delivery. HeLa-K cells were incubated with different concentration of  $E_4$ -Lipo-DOX (red circle), Lipo-DOX (black triangle) or free-DOX (open circle) for 12 h, then washed 3-time. Twenty-four hours after treatment, cell viability was measured.  $n = 4$ , error bar indicates SD. \* $P < 0.05$ .

## $E_4/K_4$ Coiled-Coil Formation Enhances Anticancer Efficacy of DOX in Xenografts

To investigate the toxicity of DOX towards cancer cells *in vivo*, we conducted another zebrafish xenograft experiment, similar to the TP3 study above. We injected HeLa-K-tdTom cells into the circulation from the duct of Cuvier at 48 hpf, followed by  $E_4$ -Lipo-DOX, Lipo-DOX or free DOX injection at 5 hpi. Twenty-four hours after DOX injection, these xenografts were imaged using fluorescent microscopy (**Figure 4A**). As illustrated by the images in Figure 4A, the fluorescence of the HeLa-K-tdTom cells was substantially more reduced by treatment with  $E_4$ -Lipo-DOX (2nd image) than by treatment with either Lipo-DOX (3rd image) or free DOX (4th image). Quantification of the fluorescent intensities showed that injection of  $E_4$ -Lipo-DOX resulted in a significantly ( $P < 0.05$ ) reduced tumor cell proliferation compared to Lipo-DOX or free DOX treatment (**Figure 4B**). Other non-targeting conditions (HeLa-K-tdTom with Lipo-DOX and free-DOX) did not exhibit significant reduction of cancer cell burden, similar to the *in vitro* experiment in **Figure 3C**.

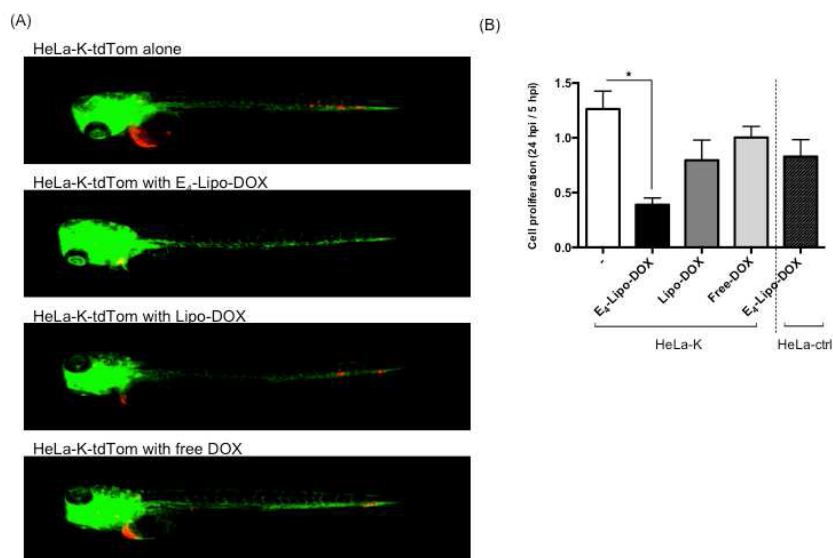


**Figure 4. E<sub>4</sub>/K<sub>4</sub> coiled coil formation enhances anti-cancer property of doxorubicin in the xenografts.** (A) HeLa-K or HeLa-ctrl cells were injected to the duct of Cuvier of 48 hpf zebrafish. After 5 h, 1 nL of 1 mM E<sub>4</sub>-Lipo-DOX, Lipo-DOX or 0.25 mM free-DOX was injected from CV, and imaged at 72 hpf. HeLa-K xenograft with E<sub>4</sub>-Lipo-DOX injection (left upper panel) shows the decrease of the injected cells. Green and red indicates vasculatures and cancer cells, respectively. (B) Quantification of the cancer proliferation in the xenografts. Cancer cell proliferation was calculated as the ratio of tdTomato fluorescence intensity in the tumour area relative to that at 5 hpi.  $n = 10 - 12$ , error bar = +SE, \* $P < 0.05$ .

As described in the Materials and Methods, we injected 1 nL of 1 mM liposomes containing 0.25 mM DOX. Based on a wet weight estimation of 240  $\mu$ g for zebrafish larvae,<sup>37</sup> the injection volume of DOX was equal to 1  $\mu$ mol /kgBW (kilogram per body weight). In the clinic, DOX is usually injected into the circulation of cancer patients at a concentration of 2.5 mg/kgBW, which equals to 5.16  $\mu$ mol /kgBW.<sup>38</sup> Therefore, the administered amount of DOX using E<sub>4</sub>-liposomes was 5-fold lower than that used in a clinical setting with lesser opportunity for exhibition of cardiac toxicity, while the anticancer efficacy of E<sub>4</sub>-Lipo-DOX is far greater than that of free-DOX.

## CONCLUSIONS

Targeted drug delivery systems should increase the efficacy of a drug and concomitant reduce the toxic side effects caused by off-target reactions. Coiled-coil motifs were recently used in a “drug free therapeutic system” to specifically kill cancer

cells.<sup>39</sup> In this study, we demonstrated that coiled coil formation between liposomes and live cells enables the *in vivo* delivery of an anticancer drug encapsulated in CPE decorated liposomes to the targeted cells in an animal model. This is one of the first examples using a synthetic coiled coil motif for *in vivo* targeted drug delivery. Although this system currently requires K<sub>4</sub> peptide expression on the cell membrane of targeted cells in zebrafish xenografts, this method can be used for animal testing of a wide range of drug candidates because of the surprising degree of functional conservation in basic cell-biological processes between zebrafish and mammals.<sup>40</sup> Furthermore, the combination of coiled coil mediated delivery and zebrafish xenografts of human cancer has the potentials to become a powerful and rapid *in vivo* drug-screening platform. For future clinical applications however, it will be necessary to introduce K<sub>4</sub> peptide to the targeted cells or tissues of interest (e.g. tumor). This might be achieved by injection of a PEGylated CPK that can be locally deshielded by irradiation with light conjugation of peptide K<sub>4</sub> peptide<sup>27</sup> to cancer-specific cell membrane antibodies (e.g. Her2 antibody<sup>41</sup>) or direct introduction of our K<sub>4</sub>-PDGFR-TMD construct using adeno-associated virus vector injection.<sup>42</sup> The proposed improvements of the current method should enable spatiotemporal control of liposomal drug targeting in the near future. These approaches to introduce K<sub>4</sub> peptide into diseased tissues or cells combined with the enhanced drug selectivity circumventing lysosomal degradation might increase the drug efficacy and reduce the toxic side effects.

## **EXPERIMENTAL PROCEDURES**

### **Materials and Methods**

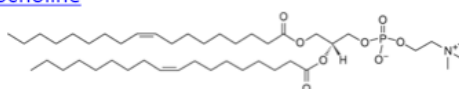
1,2-dioleoyl-sn-glycero-3-phosphocholine (DOPC), 1,2-dioleoyl-sn-glycero-3-phosphoethanolamine (DOPE) and 1,2-dioleoyl-sn-glycero-3-phosphoethanolamine-N-(7-nitro-2-1,3-benzoxadiazol-4-yl) (ammonium salt) (DOPE-NBD) were purchased from Avanti Polar Lipids. EDTA, HCTU and HOBt were purchased from Sigma Aldrich. 8-wells slide Lab-tek was purchased from Thermo Scientific, USA. DMEM medium was obtained from Gibco, life technologies. WST-1 was obtained from Serva. PMS-Ome was obtained from Santa Cruz Biotechnology. The composition of PBS is (K<sub>2</sub>HPO<sub>4</sub> (14.99 mM), KH<sub>2</sub>PO<sub>4</sub> (5 mM), and NaCl (150.07 mM) and PB is Na<sub>2</sub>HPO<sub>4</sub> (1 mM) and NaH<sub>2</sub>PO<sub>4</sub> (1 mM) at molar ratio of 5:2, pH 7.4.

## Peptide Synthesis

The cholesterol modified peptides were synthesized as described elsewhere.<sup>24</sup> Synthesis of fluorescently labelled peptides was performed on rink amide resin. After initial Fmoc deprotection using 20% piperidine in DMF, Fmoc-Lys(boc)-COOH was coupled, using 4 eq. of DIC and 4 eq. of HOBT, for 1 h. Next, the side chain Boc group was removed using TFA/ DCM (50:50 v/v) for 30 mins. The resin was then neutralized using DIPEA/NMP (10:90 v/v) for 10 mins (3x). 5(6)-Carboxyfluorescein (Sigma-Aldrich, St. Louis, MO, USA) was coupled using 4 eq. of DIC and 4 eq. of HOBT dissolved in DMF and coupling was performed overnight. The resulting fluorescently labelled resin was used to synthesize fluorescently labelled acetylated peptide E<sub>4</sub> and K<sub>4</sub> along with fluorescently labelled CPE using standard Fmoc chemistry procedure described earlier.<sup>24</sup>

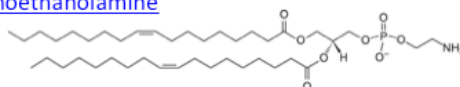
DOPC: [1,2-dioleoyl-sn-glycero-3-phosphocholine](#)

C<sub>44</sub>H<sub>84</sub>NO<sub>8</sub>P, Mw: 786.113



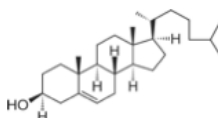
DOPE: [1,2-dioleoyl-sn-glycero-3-phosphoethanolamine](#)

C<sub>41</sub>H<sub>78</sub>NO<sub>8</sub>P, Mw: 744.034



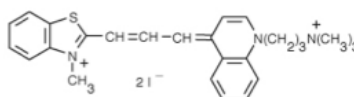
CHO: [Cholesterol](#)

C<sub>27</sub>H<sub>46</sub>O, Mw: 386.654



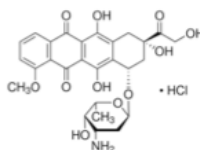
TP3: [TOPRO3 iodide](#)

C<sub>26</sub>H<sub>31</sub>I<sub>2</sub>N<sub>3</sub>S, Mw: 671.42

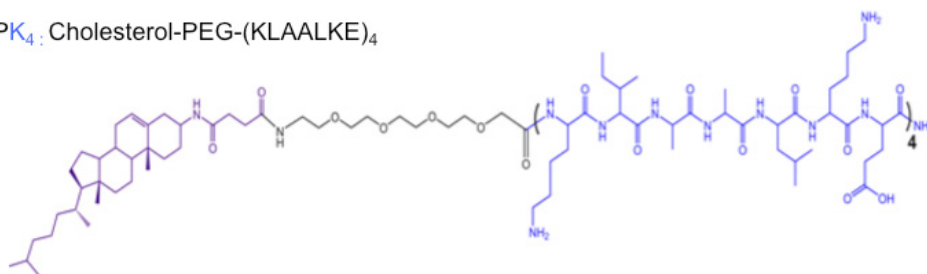


DOX: [Doxorubicin hydrochloride](#)

C<sub>27</sub>H<sub>30</sub>ClNO<sub>11</sub>, Mw: 579.98



CPK<sub>4</sub>: Cholesterol-PEG-(KLAALKE)<sub>4</sub>



CPE<sub>4</sub>: Cholesterol-PEG-(ELAALEK)<sub>4</sub>

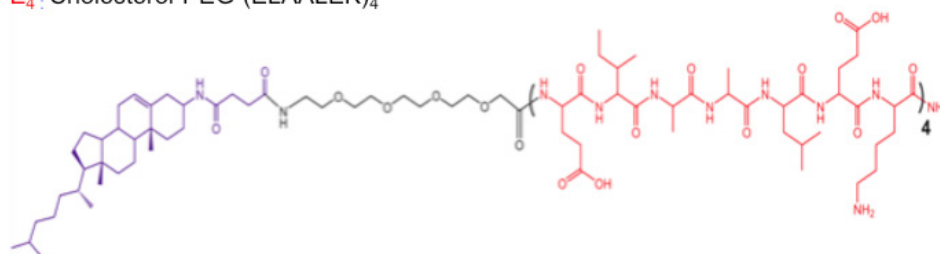


Table S1. Chemical structures of lipids, TP3, DOX, and lipopeptides CPK<sub>4</sub>, CPE<sub>4</sub>

## Peptide and Liposome Sample Preparation

DOPC, DOPE, Cholesterol and DOPE-NBD were mixed at a molar ratio 49.5:24.75:24.75:1, lipids were dissolved in CHCl<sub>3</sub>, [total lipid concentration] = 1 mM. Peptides stock solutions of 50 μM were prepared in CHCl<sub>3</sub>/CH<sub>3</sub>OH (1:1 v/v). Peptide sample was prepared by taking the appropriate amount of peptide stock, evaporating the solvent over a stream of air, addition of PBS and sonication for 1 min at 55°C, final concentration was 5 μM. Liposomes were prepared by mixing the appropriate amount of lipids plus 1 mol% of the lipidated peptides CPE<sub>4</sub> or CPK<sub>4</sub> in a 20 mL glass vial and evaporating the solvents over air pressure to form lipid films. Traces of solvent were removed under high vacuum for 3-4 h at 25°C. The lipid film was then hydrated with 0.25 mM TO-PRO-3 in PBS (Life Technologies, Carlsbad, CA, USA; after removing DMSO by freeze-drying).

For the incorporation of DOX into liposomes, the stock solutions of phospholipids (10 mM) in  $\text{CHCl}_3$  /  $\text{CH}_3\text{OH}$  (1: 1 vol%) were prepared and stored at  $-20\text{ }^\circ\text{C}$ . The stock solution were mixed to obtain the desired liposome formulation (DOPC: DOPE;CHO = 2:1:1 mol%). 1 ml stock solution was evaporated under a  $\text{N}_2$  flow and lipid film was rehydrated by citrate buffer (pH 3.5, 200 mM). The solution was vortexed for 30 sec to form a cloudy lipid suspension and sonicated in a water bath at temperature  $50\text{ }^\circ\text{C}$  for 1 h. After size exclusion by a Sephadex G25 column<sup>44</sup> with buffer PBS (  $\text{K}_2\text{HPO}_4$  (14.99 mM),  $\text{KH}_2\text{PO}_4$  (5 mM) and NaCl (100mM), pH 7.4), 2.5 ml liposome suspension were obtained. Then weighted doxorubicin were added into the liposome suspension at a mole ratio of 3: 1 and vortexed for 12 h at the temperature  $4\text{ }^\circ\text{C}$ . The resulting liposomes were stored at  $4\text{ }^\circ\text{C}$  (final lipid concentration was around 1 mM) and the hydrodynamic diameter as determined by DLS was approximately 90 nm.

### DOX Release Profile from Liposomes

The *in vitro* release of DOX from liposomes was performed at  $37\text{ }^\circ\text{C}$  to mimic the body temperature of mammals. Fresh DOX loaded liposomes were suspended in 1 ml of pre-warmed PBS (pH 7.4) and incubated at  $37\text{ }^\circ\text{C}$  in a water bath. The release amount of DOX from liposomes at different time points were collected from centrifugal Filter-100K by centrifugation (2500 rpm, 60 mins), and quantified by measuring the fluorescence of DOX ( $\lambda_{\text{Ex}}$  = 490 nm,  $\lambda_{\text{Em}}$  = 590 nm,) Ctrl+ = Fresh DOX loaded liposome with 0.5 % Triton X-100.

### Quantification of DOX Entrapment Efficiency in Liposomes

Untrapped free DOX was separated from liposomes by size exclusion chromatography (SEC) using a Sephadex G-25 column (GE Healthcare, Waukesha, WI, USA) with UV detection at 490 nm. Liposomes were collected and dissolved in 10% Triton X-100 for the content measurement of DOX in the liposomes by UV-vis spectrophotometry (Lambda 650, Perkin Elmer, Wellesley, MA, USA). The loading/entrapment efficiency (%) was calculated by dividing the amount of encapsulated drug by the total amount of added drug, multiplied by 100.



### Insert Sequence for Membrane-Expression of K<sub>4</sub> Peptide

tcgtcgacgccacc**ATG**GAGACAGACACACTCCTGCTATGGGTACTGCTGCTCT-  
GGGTTCCAGGTTCCACTGGTGACGGTGGAGGTAAAATAGCCGCACT-  
GAAGGAAAAGATCGCTGCGCTGAAGGAGAAGATTGCTGCACTCAAGGA-  
GAAAATCGCCGCCTTGAAAGAAAATGCTGTGGGCCAGGACACGCAGGAG-  
GTCATCGTGGTGCCACACTCCTTGCCCTTTAAGGTGGTGGTGATCTCAGC-  
CATCCTGGCCCTGGTGGTGCTCACCATCATCTCCCTTATCATCCTCATCATGC-  
TTTGGCAGAAGAAGCCACGT**TAG**gcgggccgcat

\* Underlines indicate Sall and NotI restriction site.

\* It contains Kozak, mouse IgK leader, K<sub>4</sub> peptide, and PDGFRB-TMB (square indicates actual transmembrane domain of PDFRRB), respectively.

### Zebrafish Strain, Husbandry, and Egg Collection

Tg (fli1: EGFP) zebrafish<sup>43</sup> were used in this study. Livestock was maintained and handled according to the guidelines from <http://zfin.org>. Fertilization was performed by natural spawning at the beginning of the light period, and eggs were raised at 28°C. All experimental procedures were conducted in compliance with the directives of the animal welfare committee of Leiden University.

### Plasmids

The insert design for membrane-expression of K<sub>4</sub> and E<sub>4</sub> peptide were described in Supplementary Methods. The insert sequences were synthesized by Base-Clear (Leiden, the Netherlands), then digested with Sall and NotI, and ligated into episomal plasmid pEBMulti-Hyg (Wako Pure Chemicals, Osaka, Japan) to create pEBM-K and pEBM-E plasmids. The backbone vector harbors OriP (replication origin) and EBNA-1 derived from Epstein-Barr Virus, which allows the distribution of this plasmids to daughter cells by episomally-replication to generate stable transformants.<sup>45</sup>

### Cells

HeLa human cervical cancer cells were obtained from the American Type Culture Collection (Manassas, VA, USA). The cells were maintained in Dulbecco's modified Eagle's medium (DMEM; Life Technologies, Carlsbad, CA, USA), supplemented with 10% fetal bovine serum (FCS; Life Technologies), 100 units/mL of penicillin (Sigma-Aldrich, St Louis, MO, USA) and 100 µg/mL streptomycin (Sigma-Aldrich) at 37°C with 5% CO<sub>2</sub>. To construct HeLa-K and HeLa-E cells, HeLa cells were transfected with pEBM-K or pEBM-E plasmid, and cultured in the presence of hygromycin B (200 µg/mL; Sigma-Aldrich) at least 2 weeks to obtain stable transformants. For control cells (HeLa-ctrl), the cells were transfected with the plasmid harboring PDGFR-TMD. For tdTomato fluorescent protein expression, the cells were infected with tdTomato lentivirus (pLenti-tdTomato-Bla; a gift from Dr. Maciej Olszewski) according to the standard protocol. The tdTomato-cells were cultured in the presence of blasticidin (10 µg/mL; Life Technologies) to obtain stable transformants.

### Cell Imaging

The cells were seeded in an 8-well slide (µ-Slide 8 well; ibidi, Munich, Germany) at a density of  $2.5 \times 10^4$  cells per well in DMEM-10% FCS medium without phenol red, and cultured overnight. Then, the medium was refreshed and added test compounds (TP3 or DOX-containing liposomes, which diluted into final concentration by DMEM (no phenol red)). After incubation for 15 min, cells were washed three times with medium. The fluorescent images were acquired using a Leica TCS SP8 confocal laser scanning microscope (Leica Microsystems, Wetzlar, Germany) and merged with Leica application suite advanced fluorescence software (Leica Microsystems) or ImageJ software (National Institutes of Health, Bethesda, MD, USA). The wavelength settings for TP3 and DOX were Ex/Em: 641/662 nm (Ex laser: 633 nm) and 480/580nm (Ex laser: 532 nm), respectively.

### Cellular Uptake Assay

HeLa-K cells were seeded in an 8-well slide at a density of  $2.5 \times 10^4$  cells per well and incubated at 37 °C in 7% CO<sub>2</sub> atmosphere. After 21 h, medium was removed and cells were incubated with 250 µl of nocodazole (40 µM), wortmannin (0.25 µM), chlorpromazine (40 µM), genistein (200 µM), or sodium azide 0.01% w/v in medium. After 3 h pre-incubation, inhibitors were removed and the cells were treated with 250 µl of CPE4-liposomes containing DOX (250 µM) in the presence of fresh inhibitors. After 15 min. liposomes and inhibitors were removed and washing steps were performed. The slide was transferred to the Leica TCS SP8 confocal laser

scanning microscope immediately and images were recorded. Image J was used for image analysis.<sup>46</sup> Wavelength setting for DOX: Ex/Em= 490/590 nm (Ex laser: 543 nm).

### Cell Viability Assay

HeLa cells were seeded in a 96-well plate at concentration of  $5 \times 10^3$  cells/well in DMEM-based complete medium and cultured overnight. E<sub>4</sub>-Lipo-DOX, Lipo-DOX or free DOX was added to the cell culture, and incubated for 12 h. After washing with DMEM containing 1% FCS for three times, the plate cells were incubated for 24 h. Then, the cell viability was measured using the CellTiter-Glo luminescent cell viability assay<sup>47</sup> (Promega, Madison, WI, USA). Luminescence signals were measured using an Infinite M1000 (TECAN, Durham, NC, USA). HeLa cells without any treatment, which was set at 100% cell survival.

### Zebrafish Xenografts and Compound Treatment

HeLa cells implantation was performed as previously reported.<sup>48</sup> In brief, dechorionized 48 hpf zebrafish were anaesthetized with 0.003% tricaine (MS222; Sigma-Aldrich). Then, trypsinized HeLa cells (100-200 cells) were injected into the duct of Cuvier by using a Pneumatic Pico pump and a manipulator (World Precision Instruments, Sarasota, FL, USA). After implantation, zebrafish were maintained at 34 °C. Five hours after implantation (hpi), 1 nL of test compounds were injected from Caudal vein using the Pico pump with fine glass needle. For live imaging, xenografts were anaesthetized and mounted in 0.6% low-melting agarose. Fluorescent image acquisition was performed using a Leica MZ16FA stereo microscope (Leica Microsystems). Images were adjusted for brightness and contrast using ImageJ.

### ACKNOWLEDGMENTS

We thank to Dr. Maciej Olszewski for giving pLenti-tdTomato-Bla lentivirus to our project. Y.S. would like to express his deep gratitude to Arwin Groenewoud for preparation of the lentivirus. J.Y. was supported with a Chinese Scholarship Council grant. A.K. acknowledges the support of NWO via a VICI grant.

## REFERENCES

1. Yu, Z.; Yan, B.; Gao, L.; Dong, C.; Zhong, J.; M, D. O.; Nguyen, B.; Hu, X.; Liang, F., Targeted delivery of bleomycin: a comprehensive anticancer review. *Curr. Cancer Drug Targets* **2015**.
2. Blume, G.; Cevc, G., Liposomes for the sustained drug release in vivo. *Biochim. Biophys. Acta, Biomembr.* **1990**, 1029, 91-97.
3. Torchilin, V. P., Recent advances with liposomes as pharmaceutical carriers. *Nat. Rev. Drug Discovery* **2005**, 4, 145-160.
4. Brock, R., The uptake of arginine-rich cell-penetrating peptides: putting the puzzle together. *Bioconjug. Chem.* **2014**, 25, 863-868.
5. Karagiannis, E. D.; Urbanska, A. M.; Sahay, G.; Pelet, J. M.; Jhunjhunwala, S.; Langer, R.; Anderson, D. G., Rational design of a biomimetic cell penetrating peptide library. *ACS Nano* **2013**, 7, 8616-8626.
6. Scott, R. C.; Wang, B.; Nallamothu, R.; Pattillo, C. B.; Perez-Liz, G.; Issekutz, A.; Del Valle, L.; Wood, G. C.; Kiani, M. F., Targeted delivery of antibody conjugated liposomal drug carriers to rat myocardial infarction. *Biotechnol. Bioeng.* **2007**, 96, 795-802.
7. Bareford, L. M.; Swaan, P. W., Endocytic mechanisms for targeted drug delivery. *Adv. Drug Delivery Rev.* **2007**, 59, 748-758.
8. Diss, M. L.; Kennan, A. J., Heterotrimeric coiled coils with core residue urea side chains. *J. Org. Chem.* **2008**, 73, 9752-9755.
9. Vandermeulen, G. W. M.; Tziatzios, C.; Klok, H.A. , Reversible self-organization of poly(ethylene glycol)-based hybrid block copolymers mediated by a de novo four-stranded  $\alpha$ -helical coiled coil motif. *Macromolecules* **2003**, 36, 4107-4114.
10. Kohn, W. D.; Mant, C. T.; Hodges, R. S., Alpha-helical protein assembly motifs. *J. Biol. Chem.* **1997**, 272, 2583-2586.
11. Lawless, M. K.; Barney, S.; Guthrie, K. I.; Bucy, T. B.; Petteway, S. R., Jr.; Merutka, G., HIV-1 membrane fusion mechanism: structural studies of the interactions between biologically-active peptides from gp41. *Biochemistry* **1996**, 35, 13697-13708.
12. Clague, M. J., Membrane transport: Take your fusion partners. *Curr. Biol.* **1999**, 9, R258-260.
13. Martelli, G.; Zope, H. R.; Capell, M. B.; Kros, A., Coiled-coil peptide motifs as thermoresponsive valves for mesoporous silica nanoparticles. *Chem. Commun. (Cambridge, U. K.)* **2013**, 49, 9932-9934.
14. Assal, Y.; Mizuguchi, Y.; Mie, M.; Kobatake, E., Growth factor tethering to protein nanoparticles via coiled-coil formation for targeted drug delivery. *Bioconjug. Chem.* **2015**, 26, 1672-1677.
15. Petrilli, R.; Eloy, J. O.; Marchetti, J. M.; Lopez, R. F.; Lee, R. J., Targeted lipid nanoparticles for antisense oligonucleotide delivery. *Curr. Pharm. Biotechnol.* **2014**, 15, 847-855.

16. Varshosaz, J.; Farzan, M., Nanoparticles for targeted delivery of therapeutics and small interfering RNAs in hepatocellular carcinoma. *World J. Gastroenterol.* **2015**, *21*, 12022-12041.
17. Pechar, M.; Pola, R.; Laga, R.; Ulbrich, K.; Bednarova, L.; Malon, P.; Sieglova, I.; Kral, V.; Fabry, M.; Vanek, O., Coiled coil peptides as universal linkers for the attachment of recombinant proteins to polymer therapeutics. *Biomacromolecules* **2011**, *12*, 3645-3655.
18. Baran, E. T.; Ozer, N.; Hasirci, V., In vivo half life of nanoencapsulated L-asparaginase. *J. Mater. Sci. Mater. Med.* **2002**, *13*, 1113-1121.
19. LaVan, D. A.; McGuire, T.; Langer, R., Small-scale systems for in vivo drug delivery. *Nat. Biotechnol.* **2003**, *21*, 1184-1191.
20. Gregory, A. E.; Titball, R.; Williamson, D., Vaccine delivery using nanoparticles. *Front Cell Infect Microbiol* **2013**, *3*, 13.
21. Kverka, M.; Hartley, J. M.; Chu, T. W.; Yang, J.; Heidchen, R.; Kopecek, J., Immunogenicity of coiled-coil based drug-free macromolecular therapeutics. *Biomaterials* **2014**, *35*, 5886-5896.
22. Zhang, R.; Yang, J.; Chu, T. W.; Hartley, J. M.; Kopecek, J., Multimodality imaging of coiled-coil mediated self-assembly in a “drug-free” therapeutic system. *Adv Healthc Mater* **2015**, *4*, 1054-1065.
23. Robson Marsden, H.; Elbers, N. A.; Bomans, P. H.; Sommerdijk, N. A.; Kros, A., A reduced SNARE model for membrane fusion. *Angew. Chem. Int. Ed.* **2009**, *48*, 2330-2333.
24. Versluis, F.; Voskuhl, J.; van Kolck, B.; Zope, H.; Bremmer, M.; Albregtse, T.; Kros, A., In situ modification of plain liposomes with lipidated coiled coil forming peptides induces membrane fusion. *J. Am. Chem. Soc.* **2013**, *135*, 8057-8062.
25. Zheng, T.; Voskuhl, J.; Versluis, F.; Zope, H. R.; Tomatsu, I.; Marsden, H. R.; Kros, A., Controlling the rate of coiled coil driven membrane fusion. *Chem. Commun. (Cambridge)* **2013**, *49*, 3649-3651.
26. Kong, L.; Askes, S. H.; Bonnet, S.; Kros, A.; Campbell, F., Temporal control of membrane fusion through photolabile PEGylation of liposome membranes. *Angew. Chem. Int. Ed.* **2016**, *55*, 1396-1400.
27. Zope, H. R.; Versluis, F.; Ordas, A.; Voskuhl, J.; Spaink, H. P.; Kros, A., In vitro and in vivo supramolecular modification of biomembranes using a lipidated coiled-coil motif. *Angew. Chem. Int. Ed.* **2013**, *52*, 14247-14251.
28. Oude Blenke, E.; van den Dikkenberg, J.; van Kolck, B.; Kros, A.; Mastrobattista, E. Coiled coil interactions for the targeting of liposomes for nucleic acid delivery. *Nanoscale* **2016**, *8*, 8955–8965.
29. Marsden, H. R.; Korobko, A. V.; van Leeuwen, E. N.; Pouget, E. M.; Veen, S. J.; Sommerdijk, N. A.; Kros, A., Noncovalent triblock copolymers based on a coiled-coil peptide motif. *J. Am. Chem. Soc.* **2008**, *130*, 9386-9393.
30. Van Hooijdonk, C. A.; Glade, C. P.; Van Erp, P. E., TO-PRO-3 iodide: a novel HeNe laser-excitable DNA stain as an alternative for propidium iodide in multiparameter flow cytometry. *Cytometry* **1994**, *17*, 185-189.

31. Szent-Gyorgyi, C.; Schmidt, B. F.; Creeger, Y.; Fisher, G. W.; Zakel, K. L.; Adler, S.; Fitzpatrick, J. A.; Woolford, C. A.; Yan, Q.; Vasilev, K. V.; Berget, P. B.; Bruchez, M. P.; Jarvik, J. W.; Waggoner, A., Fluorogen-activating single-chain antibodies for imaging cell surface proteins. *Nat. Biotechnol.* **2008**, *26*, 235-240.
32. Ono, S.; Yano, Y.; Matsuzaki, K., Improvement of probe peptides for coiled-coil labeling by introducing phosphoserines. *Biopolymers* **2012**, *98*, 234-238.
33. Evensen, L.; Johansen, P. L.; Koster, G.; Zhu, K.; Herfindal, L.; Speth, M.; Fenaroli, F.; Hildahl, J.; Bagherifam, S.; Tulotta, C.; Prasmickaite, L.; Maelandsmo, G. M.; Snaar-Jagalska, E.; Grifiths, G., Zebrafish as a model system for characterization of nanoparticles against cancer. *Nanoscale* **2015**, *8*, 862-877.
34. He, S.; Lamers, G. E.; Beenakker, J. W.; Cui, C.; Ghotra, V. P.; Danen, E. H.; Meijer, A. H.; Spaink, H. P.; Snaar-Jagalska, B. E., Neutrophil-mediated experimental metastasis is enhanced by VEGFR inhibition in a zebrafish xenograft model. *J. Pathol.* **2012**, *227*, 431-445.
35. Fritze, A.; Hens, F.; Kimpfler, A.; Schubert, R.; Peschka-Suss, R., Remote loading of doxorubicin into liposomes driven by a transmembrane phosphate gradient. *Biochim. Biophys. Acta, Biomembr.* **2006**, *1758*, 1633-1640.
36. Momparler, R. L.; Karon, M.; Siegel, S. E.; Avila, F., Effect of adriamycin on DNA, RNA, and protein synthesis in cell-free systems and intact cells. *Cancer Res.* **1976**, *36*, 2891-2895.
37. Mohan, P.; Rapoport, N., Doxorubicin as a molecular nanotheranostic agent: effect of doxorubicin encapsulation in micelles or nanoemulsions on the ultrasound-mediated intracellular delivery and nuclear trafficking. *Mol. Pharm.* **2010**, *7*, 1959-1973.
38. Hagedorn, M.; Kleinhans, F. W.; Freitas, R.; Liu, J.; Hsu, E. W.; Wildt, D. E.; Rall, W. F., Water distribution and permeability of zebrafish embryos, *Brachydanio rerio*. *J. Exp. Zool.* **1997**, *278*, 356-371.
39. Viswanatha Swamy, A. H.; Wangikar, U.; Koti, B. C.; Thippeswamy, A. H.; Ronad, P. M.; Manjula, D. V., Cardioprotective effect of ascorbic acid on doxorubicin-induced myocardial toxicity in rats. *Indian J. Pharmacol.* **2011**, *43*, 507-511.
40. Wu, K.; Yang, J.; Liu, J.; Kopecek, J., Coiled-coil based drug-free macromolecular therapeutics: in vivo efficacy. *J. Controlled Release* **2012**, *157*, 126-131.
41. Lieschke, G. J.; Currie, P. D., Animal models of human disease: zebrafish swim into view. *Nat. Rev. Genet.* **2007**, *8*, 353-367.
42. Calce, E.; Monfregola, L.; Saviano, M.; De Luca, S., HER2-mediated anticancer drug delivery: strategies to prepare targeting ligands highly specific for the receptor. *Curr. Med. Chem.* **2015**, *22*, 2525-2538.
43. Manfredsson, F. P., Introduction to viral vectors and other delivery methods for gene therapy of the nervous system. *Methods Mol. Biol. (N. Y., NY, U. S.)* **2016**, *1382*, 3-18.
44. Lawson, N. D.; Weinstein, B. M., In vivo imaging of embryonic vascular development using transgenic zebrafish. *Dev. Biol.* **2002**, *248*, 307-318.
45. Fritze, A.; Hens, F.; Kimpfler, A.; Schubert, R.; Peschka-Suss, R., Remote loading of doxorubicin

into liposomes driven by a transmembrane phosphate gradient. *Biochim. Biophys. Acta* 2006, 1758, 1633-1640.

46. Shibata, M. A.; Miwa, Y.; Morimoto, J.; Otsuki, Y., Easy stable transfection of a human cancer cell line by electroporation transfer with an Epstein-Barr virus-based plasmid vector. *Med. Mol. Morphol.* **2007**, 40, 103-107.

47. Gavet, O.; Pines, J., Progressive activation of CyclinB1-Cdk1 coordinates entry to mitosis. *Dev. Cell* 2010, 18, 533-543.

48. Luo, J.; Mohammed, I.; Warmlander, S. K.; Hiruma, Y.; Graslund, A.; Abrahams, J. P., Endogenous polyamines reduce the toxicity of soluble abeta peptide aggregates associated with Alzheimer's disease. *Biomacromolecules* **2014**, 15, 1985-1991.

## SUPPLEMENTARY FIGURES

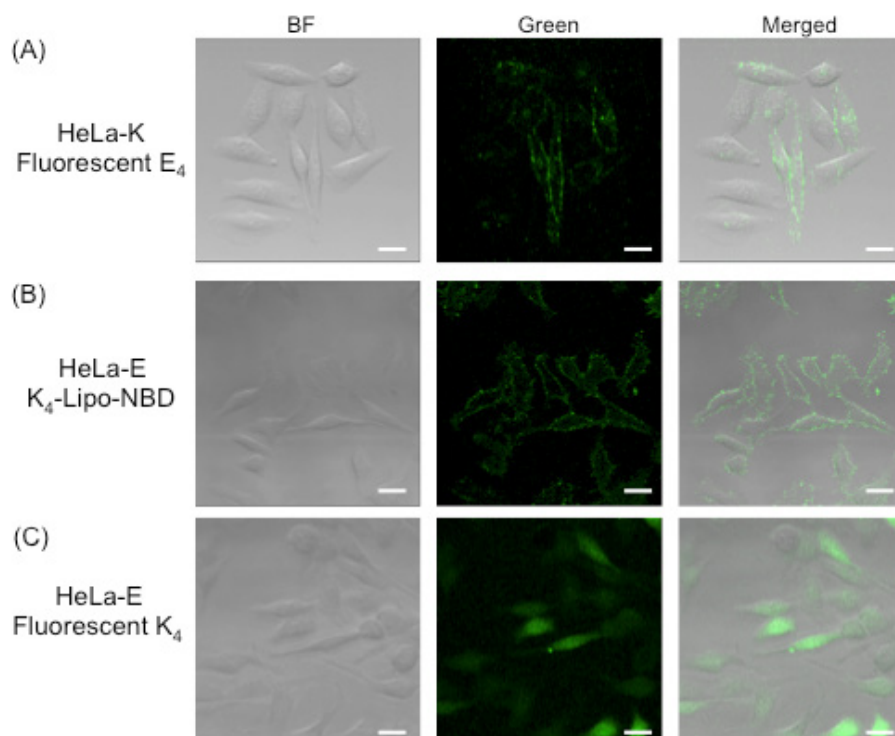


**Figure S1. Genetic expression of  $K_4$  or  $E_4$  peptide on the cell membrane.** (A) HeLa-K were treated with 5  $\mu\text{M}$  of fluorescently labeled  $E_4$  (carboxyfluorescein) for 15 min, after 3 washings with culture medium, the cells were imaged by confocal microscopy.  $K_4$  decorated liposomes containing 1% DOPE-NBD could successfully dock at the surface of HeLa-E cells (B), while fluorescently labeled  $K_4$  was able to enter HeLa-E cells (C). The scale bar represents 25  $\mu\text{m}$ .



## Application of Coiled Coil Peptides in Liposomal Anticancer Drug Delivery Using a Zebrafish Xenograft Model

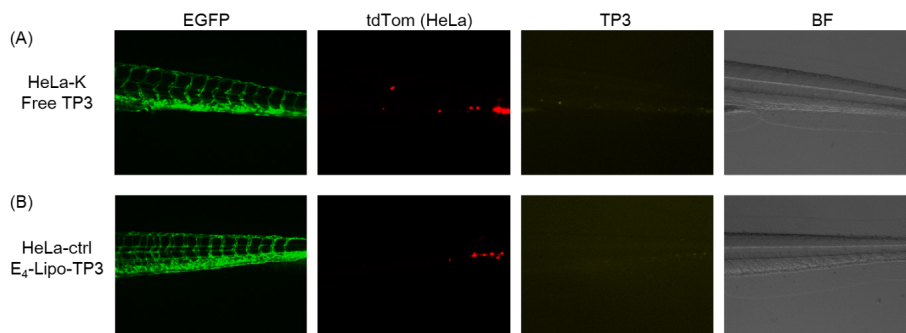


**Figure S2: Delivery of DOX relies on the coiled coil formation in xenografts.** HeLa-K or HeLa-ctrl cells (50-100 cells) were injected into the duct of Cuvier of 48 hpf zebrafish. Five hours after implantation (hpi), 1 nL of 1 mM  $E_4$ -Lipo-TP3 or 0.25 mM free TP3 was injected from CV and, imaged at 72 hpf. (A) HeLa-K xenograft injected with free TP3 and (B) HeLa-ctrl xenograft with  $E_4$ -Lipo-TP3. The scale bar represents 25  $\mu$ m.

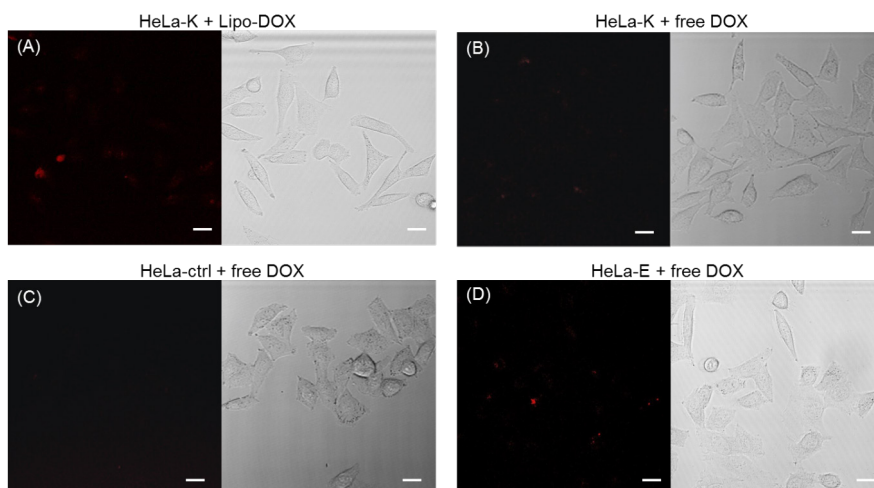


**Figure S3. Delivery of DOX relies on the coiled coil formation in vitro.** (A) HeLa-K cells were with 250  $\mu$ M Lipo-DOX for 15 mins, which diluted in DMEM (- phenol red). (B) HeLa-K cells (C) HeLa-ctrl cells (D) HeLa-E cells were treated with 15  $\mu$ M free DOX. The scale bar represents 25  $\mu$ m.

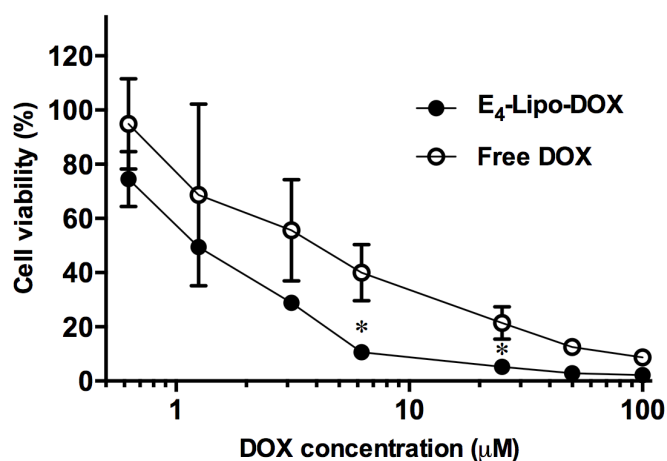


**Figure S4. Cell viability after doxorubicin delivery.** HeLa-ctrl cells were incubated with 0.25 mM E<sub>4</sub>-Lipo-DOX (closed circle), or the same concentrations of free DOX (15 μM; open circle). All cells were incubated with liposomes and/or DOX for 12 h, then were washed 3 times with medium. Twenty-four hours after treatment, cell viability was measured.  $n = 4$ , error bar indicates SD. \* $P < 0.05$ .

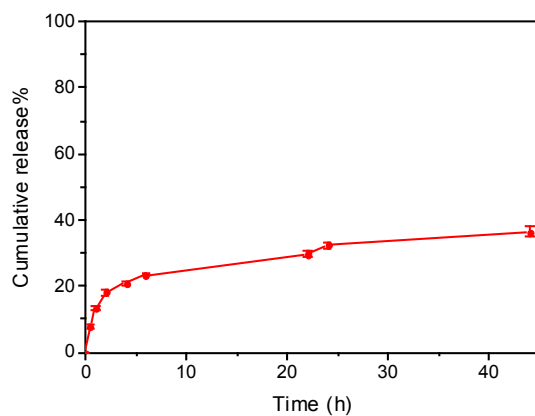


**Figure S5. Release of doxorubicin from liposomes in PBS as a function of time.**

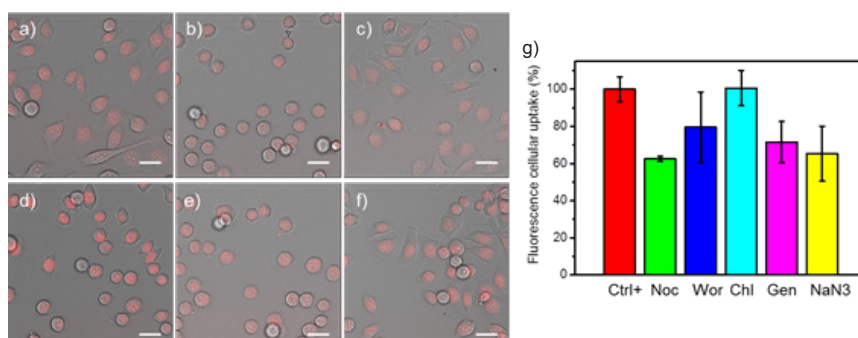


**Figure S6. Confocal images of the DOX delivery to HeLa-K cells and analysis.** HeLa-K cells were pre-treated for 3 h with a) medium (Ctrl+), or medium containing b) nocodazole (Noc) 40  $\mu$ M, c) wortmannin (Wor) 0.25  $\mu$ M, d) chlorpromazine (Chl) 40  $\mu$ M, e) genistein (Gen) 200  $\mu$ M, and f) sodium azide (NaN3) 0.1% w/v, followed by 15 min incubation with 250  $\mu$ M CPE-liposomes containing DOX, after three times washing by medium, confocal image were taken immediately. Scale bar is 25  $\mu$ m. g) Graphical representation of the percentage of DOX uptake by HeLa-K cells w/o endocytosis inhibitors. Fluorescence intensities were calculated by Image J and plotted as a percentage relative to the fluorescence of DOX in the absence of inhibitors(100%).

